Shallow Water Propagation

William L. Siegmann
Rensselaer Polytechnic Institute
110 Eighth Street
Amos Eaton 421
Troy, New York 12180-3590
phone: (518) 276-6905 fax: (518) 276-4824 email: siegmw@rpi.edu

Kara G. McMahon
Rensselaer doctoral student

Award Numbers: N000140410016, N000141310095,
N000140910638 (Ocean Acoustics Graduate Traineeship)

LONG-TERM GOALS

Develop methods for deterministic and stochastic acoustic calculations in complex shallow water environments, specify their capabilities and accuracy, and apply them to explain experimental data and understand physical mechanisms of propagation.

OBJECTIVES

(A) Treat propagation from narrowband and broadband sources over elastic and poro-elastic sediments, and incorporate realistic bathymetric, topographic, and geoacoustic variations.

(B) Quantify acoustic interactions with physical features in the ocean volume and with geoacoustic features of the ocean sediment, and analyze and interpret experimental data.

APPROACH

(A) Develop efficient and accurate parabolic equation (PE) techniques for propagation through heterogeneous sediments. Treat range dependence and sediment layering by single scattering and energy conservation methods. Benchmark results using data and special high-accuracy solutions.

(B) Construct representations for ocean environmental and geoacoustic variability using data and parametric models. Determine acoustic fields with PE, normal mode, and other approximation methods. Use experimental data and computational results to assess propagation mechanisms.

- Principal collaborators: Rensselaer PhD students, Dr. Michael Collins (NRL), Drs. James Lynch, Timothy Duda, and Ying-Tsong Lin (WHOI), Dr. Allan Pierce (BU, retired), and recent Rensselaer PhD graduates.

WORK COMPLETED

(A) Propagation model development

(1) ***Accurate calculations for range-dependent elastic media and applications***

- Validation of a recent elastic PE method, designed for problems with range-dependent bathymetry, variable thickness sediment layers, and topographic variations and for applications to beach, island, and coastal problems, is obtained [1] by comparing results from accuracy benchmarks and model environments with large sound speed changes and waves on range-dependent elastic interfaces.
- One application of the method is to shallow regions with partially consolidated sediment layers that are thin and have low shear speeds [2], which can be treated by modeling the layers as transitional interfaces and enforcing suitable conditions.
- Another application and extension is to variable ice cover in polar regions [3], where particularly strong effects on transmission loss occur when the surface ice terminates or regenerates along the propagation direction.

(2) ***New capabilities for elastic and poro-elastic sediments***

- Range-dependent transversely isotropic elastic sediments, which are a feature of coastal regions, are handled by a new PE formulation [4] that allows the significance of anisotropic effects on propagation to be evaluated.
- An initial propagation model for treating weak range dependence in transversely isotropic poro-elastic sediments [5] demonstrates that PE methods are feasible for these environments, and also indicates the influence of anisotropy.
- Propagation variables and computational techniques, designed for range-dependent elastic-layer environments, are generalized to poro-elastic sediments [6], for which computational results agree with range-independent benchmark cases and demonstrate capabilities for sediments involving both elastic and poro-elastic layers.

(B) Propagation mechanism assessment

(1) ***Specification of nonlinear internal wave effects***

- An acoustic mode propagating adiabatically across a nonlinear internal wave (NIW) at small incident angles with the wave front may produce horizontal Lloyd mirror interference patterns, as predicted and observed by other researchers, and the patterns have especially interesting features [7] when the NIW front has curvature.
- An adiabatic-mode transport theory is used to develop a scattering model for acoustic energy inside a NIW duct, in which wave front segments are treated as scattering elements [8] and a modified diffusion equation describes the evolution of averaged intensity and its dependence on environmental and acoustic parameters.
- Calculations from the modal transport theory can determine how intersecting NIW fronts influence average intensity [9], depending on the orientations of the fronts and on the asymmetry of individual scattering elements.

(2) ***Propagation dependence on attenuation in sandy-silt sediments***

- A parametric description of archetypical shallow-ocean waveguides facilitates development of new approximations for modal attenuation coefficients [10], and their frequency behavior corresponds to results of calculations for more realistic waveguides.
- Comparisons between modal attenuation coefficients obtained from Gulf of Mexico data and from new approximate formulas were performed after identifying a relevant subset of measured sound speed profiles [11], and the physical mechanism for variations in the attenuation coefficients is explained.
- Expressions for averaged transmission loss in range-independent waveguides, in terms of environmental and acoustic parameters, are derived from mode theory [12], and they reduce to well-known results of Rogers and others for high frequencies and either isospeed or constant-gradient sound speed profiles.

(3) ***Card-house structure of high-porosity marine mud***

- Electric dipoles on bubble surfaces with normally-oriented moments do not produce an interaction force between bubbles, and this conclusion, which evidently holds for non-spherical bubbles and non-strictly-normal moments [13], has implications for shapes and properties of bubbles observed in marine mud.
- A key hypothesis of the card-house model is that based on their chemical, electrical, and material structure, mud platelets behave like electric quadrupoles, so that estimates for shear wave speed can be calculated [14] by finding the effective shear modulus of the hinged joint formed by two rigid platelets, which are attached end-to-face in forming the card-house.
- Although assuming that platelets are elastic rather than rigid is a better interaction model, it is found that the calculation for the effective shear modulus leads to an unphysical singularity [15] because of the end-to-face attachment.
- The best platelet-interaction model accounts for elasticity and for end-to-face bonding across a small channel between the platelets, rather than strict attachment, and the calculation of the effective shear modulus produces shear speed estimates [16] of approximately the same size as measured for high-porosity marine mud.
- Estimates of the important parameter porosity are found by hypothesizing that card-houses grow by an idealized process (diffusion-limited cluster-cluster aggregation) that is of fractal type [17], which is validated by finding a fractal dimension for the process and comparing with results determined from observations of an aggregation experiment.

RESULTS (from two selected investigations)

(A) Accurate and efficient propagation calculations are necessary for ocean acoustic data analysis and other applications involving shallow water waveguides with range-dependent, poro-elastic sediment layers. The importance of porosity and elasticity are that they provide mechanisms to significantly change acoustic intensity and phase, by transferring energy between compressional and shear modes and by producing increased attenuation. One major computational challenge is handling sediments with relatively small values, or large changes, of geoacoustic parameters such as porosity, shear speed, and layer thickness. For poro-elastic sediments our approach employs the most widely used physical model, due to Biot. The only published poro-elastic PE has too many limitations on parameter values, even when sediment anisotropy is permitted [5]. Generalizations

of recent progress for elastic media, including accurate capabilities for complex environments with range-dependent interface waves, large changes in sediment parameters [1], and acoustically thin layers [2], are needed for layered poro-elastic sediments. These advances relied on developing different formulations for dependent variables and more accurate stair-step approximations for range-dependent sediment parameters, the latter by inserting artificial interfaces to reduce the sizes of their jumps. For poro-elastic sediments a complication is that three dependent variables are required rather than two, and effective new variables were devised for layered range-dependent environments [6]. The approach was benchmarked for multi-layered poro-elastic sediments, showing excellent agreement with results from the wavenumber integration code OASIS. In addition, the new method has capabilities that are necessary for applications and are also computationally challenging for poro-elastic sediments, such as interface waves which physically correspond to Scholte waves at water-elastic interfaces. Finally, an important feature for propagation methods is that they perform well for small or large limiting cases of geoacoustic parameter values. For instance, as shear speed values become small in elastic sediments, computational instability arises because the fluid limit is singular in the governing equations. In contrast, although the porosity dependence in the Biot sediments is complicated, on physical grounds it should not be singular. Consequently, a strenuous test for a poro-elastic PE is that results for porosity becoming small should closely approximate those from an elastic sediment. The top panel of ***Figure 1*** shows transmission loss calculations at depth 8 m for a high-frequency range-independent example, with a 1 kHz source in the middle of a 10 m fluid layer overlying a 1 m thick upper sediment layer, which in turn overlies an elastic half-space. The solid curve is the solution for a poro-elastic upper layer, with porosity 0.4 that models unconsolidated sandy sediments. The dashed curve is loss for the environment with the upper layer elastic (porosity zero) and the same parameter values as corresponding ones in the poro-elastic case. Disparities in the two curves demonstrate that the porous structure in the relatively thin upper layer significantly influences loss in the water. The middle panel is the analogous comparison when the porosity is 0.2, as in more consolidated sand. The loss patterns are still different but are smaller than in the top panel. A series of calculations were performed for decreasing porosities, and the lower panel is for the value 0.02. Here the solutions for the elastic and barely-porous layers are very close. These curves illustrate how propagation results from environments with poro-elastic layers of decreasing porosity smoothly approach those for a limiting elastic layer. Importantly, it also illustrates that the new PE solution has capabilities for accurate propagation calculations in multi-layered environments involving water and both poro-elastic and elastic sediments. Future work includes improving its capabilities, accuracy, and efficiency for range-dependent problems, along with additional benchmarking.

Figure 1 (next page). ***Propagation in layered poro-elastic sediments is accurately determined using a new PE method with a novel formulation in physical variables. Benchmarking the solution has shown its accuracy over wide ranges of geoacoustic parameter values. An important requirement for any method to handle poro-elastic sediments is that solutions for small values of porosity should approach those for an elastic sediment.***

Computations were performed for a series of range-independent environments, all with a 10 m isospeed (c_w = 1500 m/s) water layer that overlies a thin (1 m) sediment layer, which is above an elastic half-space. The geoacoustic parameters of the half-space are density ρ_s = 3.0 gm/cm^3, compressional and shear sound speeds c_p = 2400 m/s and c_s = 1200 m/s, and attenuations β_p = 0.3 dB/λ and β_s = 0.2 dB/λ In Environment A the thin layer is elastic, with ρ_s = 2.65 gm/cm^3, c_p = 1698 m/s, c_s = 119 m/s, β_p = 0.76 dB/λ , and β_s = 1.46 dB/λ . A series of N environments labeled B_N have poro-elastic thin layers, with different porosities α_N and the same values of all other Biot parameters; ρ_s , c_{p1}, β_{p1}, c_s , and β_s are the same as corresponding values in Environment A, and the slow compressional wave speed and attenuation are c_{p2} = 1023 m/s and β_{p2} = 10.2 dB/λ . The poro-elastic layer values are taken from the sand tank at the University of Texas Applied Research Laboratories. The high β_{p2} value reflects the high attenuation of the Biot slow wave.

On the next page, transmission loss (TL) curves (dB re: 1 m) are shown between 10 and 50 dB over a range of 100 m, for a 1000 Hz source at mid-depth (5 m) in the water. Figure 1(a) compares the dashed curve for Environment A and the solid curve for Environment B_1, with porosity α_1 = 0.4 corresponding to an unconsolidated sandy sediment. Both curves show multiple modes and agree in pattern for the first half of the range, with mostly higher losses from the poro-elastic layer in Environment B_1. In the second half of the range the patterns clearly differ, with Environment B_1 having peak-to-peak losses 5 to 10 dB higher than Environment A. These disparities in the curves demonstrate that the porous nature of the relatively thin upper layer (about one acoustic wavelength) significantly influences TL in the water. In Fig. 1(b) the solid curve is for Environment B_2 with thin-layer porosity α_2 = 0.2, corresponding to more consolidated sand. The solid and dashed curves have more similar patterns than in Fig. 1(a) over the entire range, with maximum peak-to-peak differences of 4 dB.

Additional results were obtained for other environments with porosity decreasing toward zero. An example is Fig. 1(c), where the solid curve from Environment B_3 has small porosity α_3 = 0.02. The TL patterns for Environments A and B3 are very close, with maximum peak-to-peak differences of about 1 dB over nearly all the range. From these and other calculations, we conclude that the new PE solutions for poro-elastic layers with decreasing porosity smoothly approach those for the limiting elastic layer. Furthermore, the method is capable of handling multi-layered ocean environments including both poro-elastic and elastic sediments.

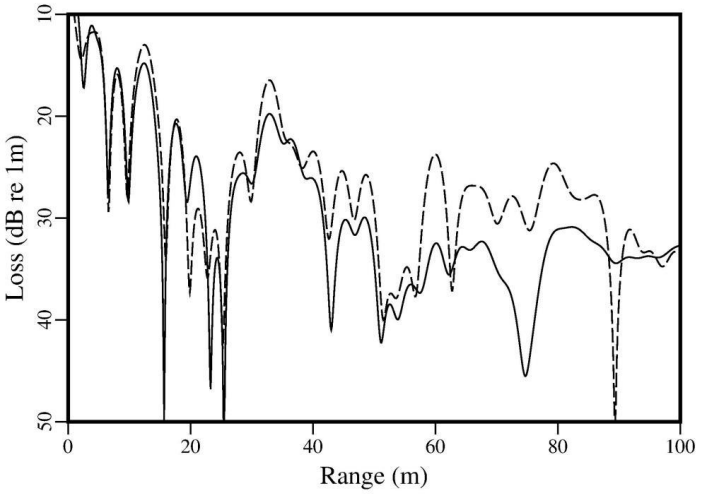
Loss (dB re 1m)
10
20
30
40
50
0
20
40
60
80
100
Range (m)

(a)

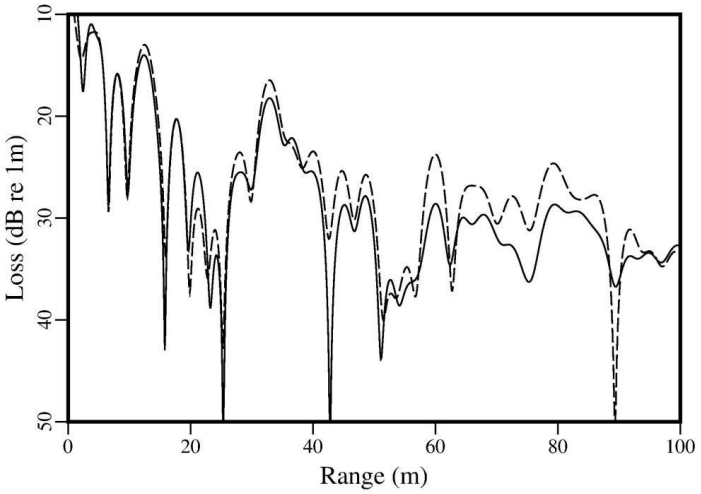
Loss (dB re 1m)
10
20
30
40
50
0
20
40
60
80
100
Range (m)

(b)

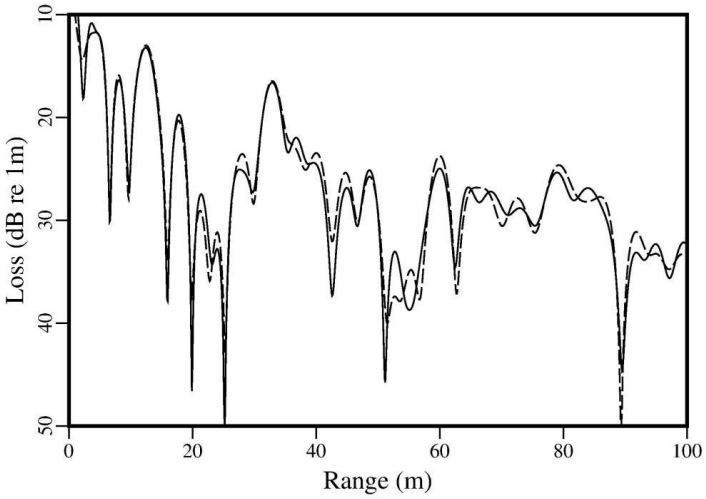
Loss (dB re 1m)
10
20
30
40
50
0
20
40
60
80
100
Range (m)

(c)

(B) Conceptual understanding and detailed knowledge of geoacoustic properties for shallow water sediments are essential for scientific and Naval applications. Sand and silt sediments have been extensively investigated experimentally and theoretically, and can be handled for propagation calculations by fluid, elastic, or poro-elastic models. In contrast for mud, and particularly for high-porosity marine mud (HPMM), none of these correctly predicts or explains all the required properties. A critical metric for success is the estimate of shear sound speed, which is low in HPMM and is not predicted by any current physically-based model. A major advance, proposed recently by Dr. Allan Pierce and the late Dr. William Carey, hypothesizes an aggregated card-house structure for HPMM. The key mechanism behind the model is the fact that each solid component, which is a thin platelet of clay minerals, has an electric charge distribution that mimics a distributed sheet of longitudinal quadrupoles that are aligned transversely to the platelet. As a result platelets repel for end-to-end or face-to-face contact, and attract end-to-face. This behavior causes the formation of card-house structures, most likely via a process called cluster-cluster aggregation that is limited by platelet diffusion. The aggregates have pores wherein bubbles may form with non-spherical shapes, which are consistent with bubble interaction properties [13]. The aggregates support weak shear stresses, and assumptions about the electrical and mechanical interactions of platelets permit estimates of the effective shear modulus and shear speed c_s. The effective shear modulus of an aggregate is found for its constituent subunits, which consist of two interacting platelets. The top left panel of ***Figure 2*** illustrates the two-platelet interaction, and as suggested by the schematic, the platelets are allowed to bend (slightly) because of their (high) elastic modulus [15]. Between the platelets a small channel of thickness d, smaller than the platelet thickness h, is hypothesized that enables ions to assist in bonding the platelets. Variations in the direction parallel to the line of interaction (the y-axis) are neglected, so that standard Euler-Bernoulli bean theory can be applied in the x-z plane. The top right panel illustrates a side view of the subunit. A shearing force F is applied at the end of one platelet, producing a small shear displacement $u(z)$ in the x-direction. The platelet is maintained in static equilibrium by distributed electrical moments $m_E(z)$ and by internal forces and moments. Beam theory leads to a third-order differential equation for $u(z)$, along with physically-based boundary conditions at the platelet ends. For relevant parameter values, the solution shows that the displacement acts as if the beam were rigid for most of the platelet [14]. That is, the electric quadrupole moment dominates the internal elastic moment, except near the channel $z = d$ where the beam must bend to satisfy the interaction conditions [16]. From the maximum displacement the shear strain due to the shear force can be found, and then the shear modulus, and finally the shear speed. The middle panel shows the expression for c_s in terms of mud density, three physical constants, and six platelet parameters. For those six, realistic variations in the values of three have little influence on the estimate of c_s, while the other three – platelet thickness h, length L, and cation exchange capacity χ – have variations that do influence c_s . The bottom panel is a table in which the second column has representative values for these three quantities, for the most common types of clay minerals in HPMM. For these minerals, kaolinite and smectite, the corresponding shear speed estimates are 13 m/s and 0.25 m/s. The third and fourth columns of the table show typical measured or estimated ranges of variability for the three quantities, and the sensitivity of c_s estimates to their variations. It is important to note that actual HPMM consists of more than one type of mineral, so that its effective shear speed would be a weighted average of those from its component minerals. We conclude from results including those in the table that shear speed estimates are consistent with values of order 10 m/s that have been measured for HPMM. Therefore, the card-house theory satisfies one critical test for its applicability. Future work includes refining predictions of porosity [17] and formulating estimates for compressible and shear attenuations.

Figure 2 (next page). *The card-house theory for the structure of high-porosity marine mud can provide estimates for key geoacoustic parameters, including shear and compressional sound speed and porosity. In particular, low estimates for shear speed are found as observed in data. The mineral constituents of mud are modeled as thin platelets with transverse length and width L, thickness h, and small aspect ratio $\delta = h/L$. In seawater their electrical properties resemble sheets of uniformly-distributed longitudinal quadrupoles that are aligned transversely to the platelet. Consequently, platelets repel face-to-face and end-to-end but attract face-to-end, which causes card-house like structures to form by an aggregation process and to support shear stresses. The effective shear modulus of the structure is approximated by that of its constituent subunits, consisting of two interacting platelets.*

Fig. 2(a) *shows a 3-D schematic of an idealized subunit, comprised of a platelet nearly vertical (the z-axis) that interacts along the center line (the y-axis) of a horizontal platelet. The platelets have a large elastic modulus E so they may bend slightly. A small gap of width d, less than h, is hypothesized between the interacting platelets to facilitate bonding. No variation is assumed in the y-direction, so the interaction can be analyzed in the x-z plane.*

Fig. 2(b) *shows a schematic side view in the z-z plane of two interacting platelets. The subunit responds to a force F in the positive x-direction with a small shear displacement u(z). The subunit is maintained in static equilibrium by distributed moments per unit length $m_E(z)$ arising from the electrical forces of the quadrupoles and by internal forces and moments. Euler-Bernoulli beam theory leads to a third-order differential equation for u(z) with boundary conditions at $z = d$ (above the gap) and $z = L + d$. Solving for the displacement shows that it corresponds to a rigid approximation for most of the platelet. Therefore, the electrical response to the quadrupoles dominates the response to the internal elastic forces, except near the gap where the beam must bend to satisfy the interaction boundary conditions.*

Fig. 2(c) *is the expression for the shear speed c_s of high-porosity marine mud from the card-house theory. The factor multiplying the square root arises from the quadrupole moment per unit area on the platelet. This factor includes two physical constants, Avogadro's constant N_A and electron charge e, plus four platelet parameters: density $\rho_{platelet}$, thickness h, cation exchange capacity χ, and the inverse e-folding distance κ of its electric field. The quantity under the square root, which is the rest of the shear modulus divided by mud density ρ_{mud}, has the permittivity of seawater ε and two more platelet parameters: length L and gap width d, taken as $\kappa^{(-1)} \approx 0.45$ nm. Of the six platelet parameters, physically meaningful variations in values of only three of them (h, L, and χ) can significantly influence c_s.*

Fig. 2(d) *is a table with h, L, χ, and c_s in its first column. The second column shows a representative value for each parameter in two clay minerals, kaolinite and smectite, which are the most common types in marine mud. These values produce 13 m/s for kaolinite and 0.25 m/s for smectite. The third column shows typical ranges of values for h, L, and χ in the two clay types. The fourth column shows the range of c_s values using the range of values for one parameter and the representative values for the others. Over all rows in column four, c_s varies from 3 to 41 m/s for kaolinite, and from 0.01 to 2 for smectite. Mud consisting of more than one type of mineral is expected to have a shear speed that is a weighted average of those from its constituents. We conclude that estimates for the shear speed of high-porosity marine mud from the card-house theory are consistent with values of order 10 m/s that have been measured.*

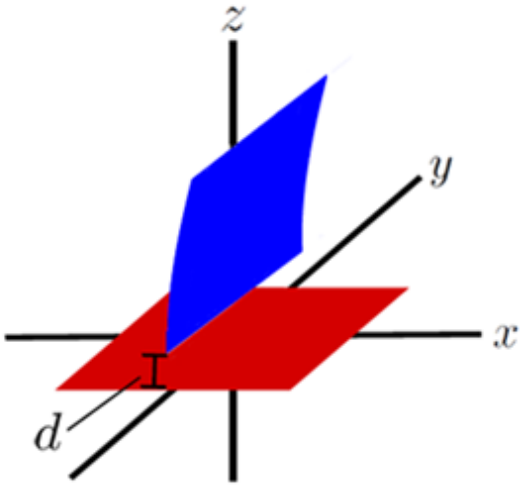

(a)

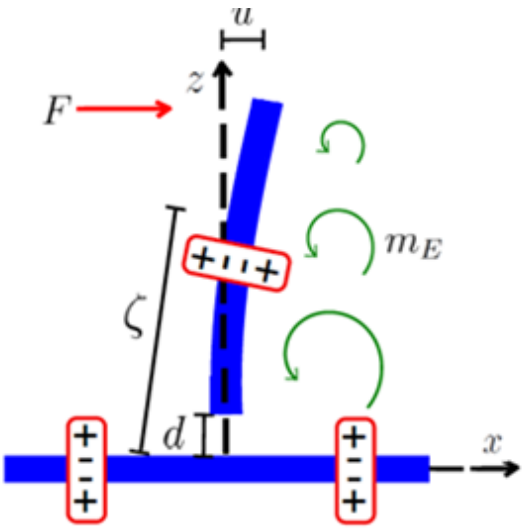

(b)

$$c_s = \frac{N_A e}{6} \rho_{platelet}\, \chi \left[\left(1 + \frac{3}{\kappa h}\right)^2 + \frac{3}{(\kappa h)^2} \right] h^3 \sqrt{\frac{1}{2\pi\varepsilon L^3 d \rho_{mud}}}$$

(c)

PAMAMETERS	Representative Value	Range of Values	Range of c_s Values
Platelet Thickness	Kaolinite: 0.05	0.03 – 0.07	**3 – 34**
h (microns)	Smectite: 0.0055	0.001 – 0.01	**0.01 – 2**
Platelet Width	Kaolinite: 0.9	0.5 – 1.3	**6 - 41**
L (microns)	Smectite: 0.9	0.5 – 1.3	**0.15 – 1**
Cation Exchange Capacity	Kaolinite: 0.09	0.03 – 0.15	**4 - 22**
χ (moles/kg)	Smectite: 1.2	0.8 – 1.5	**0.2 – 0.3**
Shear Speed	**Kaolinite: 13**		
c_s (m/sec)	**Smectite: 0.25**		

(d)

IMPACT/APPLICATIONS

New or enhanced capabilities are provided for propagation predictions that depend on physical properties of shallow water sediments, including layering, elasticity, porosity, and anisotropy. Range-dependent variability from bathymetry, topography, and sediment interfaces can be treated in propagation calculations. Intensity attenuation and coherence statistics that result from environmental fluctuations and other experimental variability can be found more efficiently. Data analyses and model comparisons allow specification of the roles of key physical mechanisms, such as linear or nonlinear frequency dependence of sediment attenuation, sediment heterogeneity or homogeneity, water column or bathymetric variability, water column scattering or refraction, and vertical or horizontal mode coupling from nonlinear internal waves and bathymetry. Results from modeling and data analyses of experiments, particularly experiments off the New Jersey Shelf, are partly aimed at improving shallow water sonar systems and predictions. Propagation model implementations, analysis tools, and data representation techniques are distributed to university, laboratory, and other research/development groups.

RELATED PROJECTS

- Continuing projects with Dr. Michael Collins include [4], extensions of [6], and a monograph on new parabolic wave equation models and applications [19], for which the principal research results are nearly complete.

- In addition to investigations with Drs. James Lynch, Y.-T. Lin, and Timothy Duda [9]-[11] of propagation effects from waveguides generated by nonlinear internal waves, other projects are under way, including extensions of curvature effects in internal wave ducts [18]. Research under this grant is related to the WHOI-led MURI project, "Integrated Ocean Dynamics and Acoustics."

- Current research with Dr. Allan Pierce [13]-[17] focuses on propagation variability from sediment geoacoustic structure and attenuation, and on quantifying structural and acoustic predictions from his card-house theory of high-porosity marine mud.

REFERENCES

[1] A. M. Metzler, W. L. Siegmann, M. D. Collins, and J. M. Collis, "Single-scattering parabolic equation solutions for elastic media propagation, including Rayleigh waves," *J. Acoust. Soc. Am.,* **131**, 1131-1137 (2012).

[2] J. M. Collis, A. M. Metzler, and W. L. Siegmann, "Seismo-acoustic propagation for thin and low shear speed ocean elastic sediments." See also (A) *J. Acoust. Soc. Am.,* **132**, 1973 (2012). In preparation for submission.

[3] A. M. Metzler, J. M. Collis, and W. L. Siegmann, "Low-frequency seismo-acoustic propagation under variable ice over in the Arctic using a parabolic equation." See also (A) *J. Acoust. Soc. Am.,* **132**, 1974 (2012). In preparation for submission.

[4] A. M. Metzler, W. L. Siegmann, M. D. Collins, and J. M. Collis, "Parabolic equation solutions for anisotropic waves in heterogeneous media." In preparation for submission.

[5] A. J. Fredricks, W. L. Siegmann, and M. D. Collins, "Parabolic equation models for anisotropic poro-elastic media." Submitted for refereed publication.

[6] A. M. Metzler, W. L. Siegmann, M. D. Collins, and J. M. Collis, "Two parabolic equations for propagation in layered poro-elastic media," *J. Acoust. Soc. Am*. **134**, 246-256 (2013).

[7] K. G. McMahon, L. K. Reilly-Raska, W. L. Siegmann, J. F. Lynch, and T. F. Duda, "Horizontal Lloyd Mirror patterns from straight and curved nonlinear internal waves," *J. Acoust. Soc. Am.*, **131**, 1689-1700 (2012). Supported by OA Graduate Traineeship Award 0638.

[8] K. G. McMahon, J. F. Lynch, Y.-T. Lin, W. L. Siegmann, and N. Xiang, "Energy transport in nonlinear internal wave ducts." See also (A) *J. Acoust. Soc. Am*. **128**, 2335 (2010). In preparation for submission. Supported by OA Graduate Traineeship Award 0638.

[9] K. G. McMahon, J. F. Lynch, Y.-T. Lin, N. Xiang, and W. L. Siegmann, "Nonlinear internal wave influence on energy propagation using transport theory." See also (A) *J. Acoust. Soc. Am*. **129**, 2458 (2011). In preparation for submission. Supported by OA Graduate Traineeship Award 0638.

[10] W. J. Saintval, A. D. Pierce, W. M. Carey, and W. L. Siegmann, "A modified Pekeris waveguide for examining sediment attenuation influence on modes." Submitted for refereed publication.

[11] W. J. Saintval, W. L. Siegmann, W. M. Carey, and A. D. Pierce, "Parameter sensitivities of modal attenuation coefficients for sandy sediments in the Gulf of Mexico." Submitted for refereed publication.

[12] S. V. Kaczkowski, A. D. Pierce, W. M. Carey, and W. L. Siegmann, "Averaged transmission loss expressions in shallow water waveguides with sandy-silty sediments." See also (A) *J. Acoust. Soc. Am*. **128**, 2480 (2010). In preparation for submission.

[13] J. O. Fayton, A. D. Pierce, W. M. Carey, and W. L. Siegmann, "The card-house structure of mud: Influence of particle interaction energy on bubble formation and growth." See also (A) *J. Acoust. Soc. Am*. **127**, 1938 (2010). In preparation for submission.

[14] J. O. Fayton, A. D. Pierce, W. M. Carey, and W. L. Siegmann, "The card-house structure of mud: Determination of shear wave speed." See also (A) *J. Acoust. Soc. Am*. **128**, 2357 (2010).

[15] J. O. Fayton, A. D. Pierce, W. M. Carey, and W. L. Siegmann, "The card-house structure of mud: Estimation of shear wave speed in mud with elastic platelets." See also (A) *J. Acoust. Soc. Am*. **129**, 2389 (2011).

[16] J. O. Fayton, A. D. Pierce, and W. L. Siegmann, "Electrochemical basis of the card-house model of mud and its acoustical implications." See also (A) *J. Acoust. Soc. Am*. **133**, 3305 (2013). In preparation for submission.

[17] J. O. Fayton, *"Estimates of Geoacoustic Parameters of Marine Mud,"* Ch. 3: "Platelet aggregation and estimation of porosity from computational fractal modeling," Ph.D. thesis, Rensselaer Polytechnic Institute, to be defended November 2013. In preparation for submission.

[18] Y.-T. Lin, K. G. McMahon, W. L. Siegmann, and J. F. Lynch, "Horizontal ducting of sound by curved nonlinear internal gravity waves in the continental shelf areas," *J. Acoust. Soc. Am*. **133**, 37-49 (2013). Supported by OA Graduate Traineeship Award 0638.

[19] M. D. Collins and W. L. Siegmann, *Parabolic Wave Equations with Applications*. In preparation for Springer-Verlag publishers.

PUBLICATIONS

- Published [refereed]: [1], [6], [7], [18]
- Submitted [refereed]: [5], [10], [11]